Cell Host & Microbe
Short Article

The Host Nonsense-Mediated mRNA Decay Pathway Restricts Mammalian RNA Virus Replication

Giuseppe Balistreri,[1,8,*] Peter Horvath,[2,3] Christoph Schweingruber,[4,5] David Zünd,[4] Gerald McInerney,[6] Andres Merits,[7] Oliver Mühlemann,[4] Claus Azzalin,[1] and Ari Helenius[1]
[1]Institute of Biochemistry, ETH Zürich, 8093 Zürich, Switzerland
[2]Synthetic and System Biology Unit, Biological Research Center, 6726 Szeged, Hungary
[3]FIMM Institute, University of Helsinki, 00014 Helsinki, Finland
[4]Department of Chemistry and Biochemistry, University of Bern, 3012 Bern, Switzerland
[5]Graduate School for Cellular and Biomedical Sciences, University of Bern, 3012 Bern, Switzerland
[6]Department of Microbiology, Tumor and Cell Biology, Karolinska Institutet, 17177 Stockholm, Sweden
[7]Institute of Technology, University of Tartu, 50090 Tartu, Estonia
[8]Present address: Institute of Biotechnology, University of Helsinki, 00790 Helsinki, Finland
*Correspondence: giuseppe.balistreri@helsinki.fi
http://dx.doi.org/10.1016/j.chom.2014.08.007

SUMMARY

In addition to classically defined immune mechanisms, cell-intrinsic processes can restrict virus infection and have shaped virus evolution. The details of this virus-host interaction are still emerging. Following a genome-wide siRNA screen for host factors affecting replication of Semliki Forest virus (SFV), a positive-strand RNA (+RNA) virus, we found that depletion of nonsense-mediated mRNA decay (NMD) pathway components Upf1, Smg5, and Smg7 led to increased levels of viral proteins and RNA and higher titers of released virus. The inhibitory effect of NMD was stronger when virus replication efficiency was impaired by mutations or deletions in the replicase proteins. Consequently, depletion of NMD components resulted in a more than 20-fold increase in production of these attenuated viruses. These findings indicate that a cellular mRNA quality control mechanism serves as an intrinsic barrier to the translation of early viral proteins and the amplification of +RNA viruses in animal cells.

INTRODUCTION

Among innate cellular mechanisms that limit virus infection at the level of individual cells, there are some that are always present and capable of restricting incoming viruses instantly after entry. These processes are constitutive, i.e., they do not need induction by the virus or external ligands, and they are not necessarily amplifiable (Yan and Chen, 2012). Although still incompletely understood, the intrinsic immunity encompasses many different molecular strategies. In general, they seem to depend on cellular factors that detect "nonself" features in the incoming virus particles or in their components.

Focusing on the host cell entry of two arthropod-borne alphaviruses with positive-strand RNA (+RNA), Semliki Forest virus (SFV) and Sindbis virus (SINV), our current studies suggest that one of the intrinsic pathways involves nonsense-mediated mRNA decay (NMD). NMD is a well-studied process responsible for quality control and regulation of cellular mRNA molecules by rapid degradation (Kervestin and Jacobson, 2012; Lykke-Andersen and Bennett, 2014; Schweingruber et al., 2013). Cellular mRNAs that have premature stop codons or a long 3′ UTR are recognized by components of the NMD pathway and targeted for degradation.

Like other +RNA viruses, alphaviruses have a genome capable of acting as an mRNA. After delivery into the cytosol of host cells, the genomic RNA serves as a polycistronic messenger RNA for the synthesis of nonstructural viral proteins (nsPs) including RNA-dependent RNA polymerases (RdRP), helicases, and proteases. The newly synthesized nsPs associate with their own messenger and proceed to synthesize a complementary negative-stranded RNA (−RNA) that in turn serves as template for further +RNA synthesis. The amplification of viral genome is necessary for successful production of progeny virus particles a few hours later (scheme in Figure 1A). The structural proteins are translated later from a more abundant, subgenomic mRNA comprising the 3′-terminal one-third of the genomic RNA. One of the consequences of this replication strategy is that the genomic RNA used to translate the nsPs has an untranslated 3′ UTR much longer than typical for cellular mRNAs.

RESULTS

siRNA Screen Identifies UPF1 as a Restriction Factor for SFV

The starting points for our studies were automated, image-based, genome-wide siRNA screens against cellular host factors involved in the infection of various RNA and DNA viruses, including SFV as the only +RNA virus. Three days after siRNA treatment, HeLa cells were infected with a previously characterized recombinant SFV (SFV-ZsG), in which the bright green fluorescent protein ZsGreen is fused with the replicase protein nsP3 (nsP3-ZsG) (Figure 1A) (Spuul et al., 2010).

nsP3-ZsG was detected in the cytoplasm of infected cells by fluorescence microscopy as bright spots that increased with

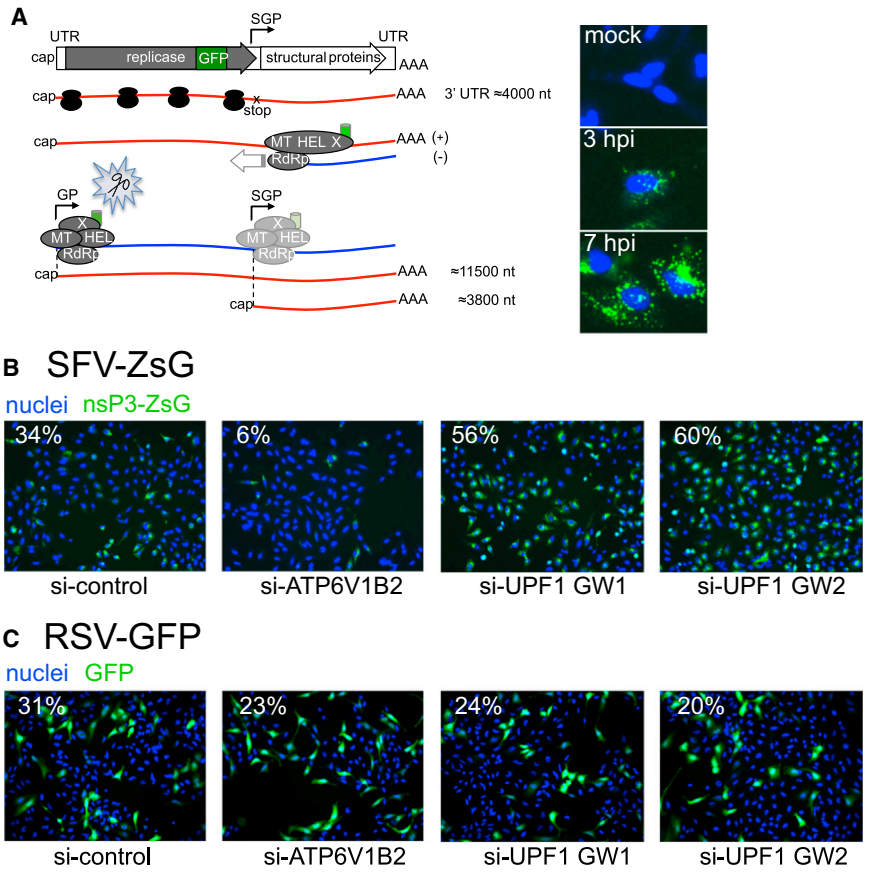

Figure 1. Genome-wide siRNA Screen Identifies Upf1 as a Restriction Factor for SFV

(A) Schematic representation of the SFV genome, viral gene expression, and genome replication. The ZsG marker gene is indicated in green. Translation of the +RNA genome gives rise to the viral replicase complexes, which subsequently produce the complementary −RNA. The −RNA is in turn used to amplify the RNA genome and to transcribe the subgenomic RNA. Proteolytic processing of the replicase determines the switch from − to +RNA synthesis. Right panel shows images of SFV-ZsG-infected HeLa cells at different times of infection (blue, nuclei; green, nsP3-ZsG).

(B and C) Representative images from the SFV (B) and RSV (C) RNAi screen; the percentage of infected cells is indicated in white and the targeted genes are indicated below each image. For Upf1, images from two independent repetitions are shown (GW1 and GW2) (see also Figure S1).

time in number, brightness, and size (Figure 1A, right panel; Figure S1). The punctate pattern allowed us to detect infection after only 3 hr. In the screen, the multiplicity of infection (moi) was adjusted so that 6 hr after infection 30% of cells treated with control siRNA were positive for the ZsG fluorescence. This allowed detection of siRNA-induced inhibition as well as elevation of infection. The screen was repeated two times independently (Figure S1B).

Depletion of Upf1 Elevates SFV Replication

Among the strongest hits that increased SFV infection after siRNA depletion, we found Upf1 (Figure S1B), an ATP-dependent RNA and DNA helicase that during translation interacts with initiation factors and the terminating ribosome (Cheng et al., 2007; Isken et al., 2008; Kashima et al., 2006) and accumulates on the 3′ UTR of mRNAs (Hogg and Goff, 2010; Hurt et al., 2013; Zünd et al., 2013). It is a central component in NMD.

siRNAs against UPF1 increased the fraction of infected cells from 34 to 56 and 60% in independent experiments (Figures 1B and S1B). Depletion of subunits of the vacuolar ATPase (V-ATPase) strongly decreased infection, as expected of a virus dependent on low pH activation for penetration (Helenius et al., 1980; White and Helenius, 1980). UPF1 was not a hit in the screen for respiratory syncytial virus (RSV, paramyxoviridae), a −RNA virus (Figure 1C), and Uukuniemi virus (Bunyaviridae), another −RNA virus (Meier et al., 2014).

To rule out off-target effects, we repeated the infection assay using a previously validated shRNA against UPF1 expressed from a plasmid that allows puromycin selection of transfected cells (Azzalin and Lingner, 2006; Paillusson et al., 2005). The depletion of Upf1 was efficient as determined by western blot analysis in parallel noninfected cultures (Figure 2B) and led to a 4-fold increase in the number of ZsG-positive cells (Figures 2A and 2C). This effect was partially reversed by expression of shRNA-resistant HA-tagged wild-type (WT) Upf1, but not by expression of an ATPase-inactive Upf1 mutant (Figure S2D). Immunofluorescence (IF) microscopy after staining with antibodies against dsRNA (a hallmark of +RNA replication) and the E1/E2 SFV glycoproteins showed a corresponding increase in replicating viral RNA (Frolova et al., 2010; Spuul et al., 2010) and in structural proteins synthesized from the subgenomic, late viral mRNA (Figures 2A and 2C). It was evident that in the absence of Upf1, all intracellular stages of SFV-ZsG and WT SFV infection were amplified.

The effect of Upf1 depletion was further confirmed using a recombinant SFV in which the ZsG was exchanged for the renilla luciferase (Rluc) enzyme (Pohjala et al., 2011). This recombinant virus provided a sensitive readout for infection at even earlier stages. As shown in Figure 2D, a 2-fold increase in signal over background was detected already 1 hr after infection. Three hours later, the signal was 6-fold higher than in controls.

Using IF with the dsRNA-specific antibodies, we tested whether SINV, another alphavirus distantly related to SFV, was also sensitive to Upf1 levels. At 4 hr after infection, the dsRNA signal in Upf1-depleted cells increased almost 4-fold over controls (Figure 2E). Thus, Upf1 counteracted the replication and amplification of viral RNA, and the effect was seen for another alphavirus as well.

When the production of progeny viruses was analyzed 24 hr after infection, it was clear that Upf1 depletion allowed a 3-fold increase in the titer of WT SFV. For the recombinant viruses SFV-Rluc and SFV-ZsG the increase was even higher (Figure 2G). We concluded that Upf1 interferes with early cytosolic

steps in alphavirus infection. It reduces the replication of viral RNA, the synthesis of nonstructural and structural proteins, and the production infectious virions.

To exclude possible effects of Upf1 depletion on virus entry, we used two assays. In the first, virus endocytosis was bypassed by acidification of the extracellular medium. This allows cell surface bound SFV to fuse directly with the plasma membrane and infect the cell (Helenius et al., 1980) (Figure S2A). As a control, we pretreated parallel cell cultures with bafilomycin-A1, an inhibitor of the vATPase responsible for endosomal acidification and virus penetration. While the effect of bafilomycin-A1 was efficiently reverted by the acidic bypass treatment, the depletion of Upf1 still resulted in increased levels of SFV infection (Figure 2F).

In the second assay, we monitored the increased exposure of the viral capsid protein (C-protein) to antibodies after loss of viral envelope and uncoating of the incoming capsid. We allowed viruses to be internalized by endocytosis for 40 min and used IF to localize the C-protein. Cycloheximide was present to inhibit viral protein synthesis. While we could readily record an increase in the fluorescence signal of the C-protein with increasing amounts of viruses added (Figures S2A–S2C), no detectable difference was observed in cells depleted of Upf1 (Figure S2C). This indicated that Upf1 restricts a process in infection occurring after penetration of the viral capsids into the cytosol and after their uncoating.

Considering what is known about Upf1, it seemed likely that the steps in question involved detection and degradation of the viral +RNA prior to or after initial translation of nsPs and the formation of viral RNA replication complexes. To test this possibility, we measured the half-life ($t_{1/2}$) of viral RNA genomes delivered to the cytoplasm by incoming viruses, in cells that were pretreated with shRNA against UPF1 or luciferase as control. The viral genomes were detected by a recently optimized single-molecule resolution fluorescent in situ hybridization (FISH) technique, in which the target RNA is hybridized to a series of "branched" DNA probes, each conjugated to a fluorophore (Battich et al., 2013) (Figure 2H).

To prevent viral RNA replication, a prerequisite for measuring the half-life of the initial viral RNA, we used a previously characterized conditional SFV mutant (Ts9) in which a point mutation in the helicase domain of nsP2 (G389R) causes a reduction of RNA replication and transcription from a WT level at 28°C to 0.5% at 39°C (Keränen and Kääriäinen, 1974, 1979). The ts-phenotype is due to loss of function in the polyprotein containing nsP1–nsP3 (Balistreri et al., 2007). When 40°C was used as the restrictive temperature, complete inhibition of replication was observed (not shown).

To obtain synchronous infection, Ts9 viruses were first bound to the surface of cells on ice and subsequently allowed to penetrate by shifting the cultures to the restrictive temperature for different periods of time. After fixation and FISH, cells were imaged by automated microscopy. Single viral genomes appeared as bright puncta in the cytoplasm of infected cells (Figure 2H). The number of puncta per cell decreased over time with exponential kinetics. The estimated half-life of the genomic viral RNAs was 63 min in cells pretreated with shRNA control. Depletion of UPF1 increased the half-life value on average by 40% ($t_{1/2}$ = 89 min) (Figures 2I and S2E). This indicated that that the incoming viral RNA was undergoing degradation and that a substantial part of this degradation involved Upf1.

Impaired Viral RNA Replication Increases Sensitivity to Upf1

If early events such as the initial translation of nsPs and the replication of the viral genome were repressed by Upf1, we expected Upf1 depletion to be especially advantageous for viral mutants compromised in these functions. First, we tested the conditional SFV mutant Ts9. For sensitive detection of viral nonstructural protein production, the Rluc gene was added to the C terminus of the nsP3 sequence of both Ts9 and WT SFV (Pohjala et al., 2011). To obtain a minimal but detectable level of virus replication, the temperature of infection was adjusted to 36°C. At this temperature, the luciferase count reached 20% of WT virus (Figure 3A). Although still detectable by IF, the accumulation of dsRNA in Ts9-infected HeLa cells was severely impaired (Figure 3B).

When Upf1-depleted cells were infected with Ts9-Rluc under these conditions, the number of cells expressing detectable dsRNA, nsP3-Rluc, and viral glycoproteins E1 and E2 was elevated up to 15-fold in HeLa cells and 30-fold in human primary fibroblasts (HPF) over control cells (Figures 3C and 3D). This prompted us to test whether the depletion of Upf1 could be used to rescue production of a strongly attenuated, nonconditional virus mutant. A recently developed SFV mutant (delta 789) was tested in which a deletion of a C-terminal fragment of nsP3 causes a 100-fold drop in virus production (Panas et al., 2012). Indeed, depletion of Upf1 caused the titer to increase up to 20-fold (Figure 3E). Thus, the Upf1-suppression effect is particularly strong when the SFV RNA helicase and nsP3 protein are compromised. It seemed likely that Upf1 prevented replication and thus amplification of the viral genome by activating viral RNA degradation.

NMD Factors Smg5 and Smg7 Restrict SFV Infection

In mammalian cells, Upf1 is a core factor of NMD but not the only necessary component (Chang et al., 2007). In the screen, the siRNA depletion of other important NMD components did not have an effect strong enough to pass the stringent criteria for "hit" definition. To test whether other NMD components were involved in inhibiting SFV replication, we employed the shRNA transfection system (Brummelkamp et al., 2002) combined with puromycin selection to deplete endogenous proteins. We used both WT SFV and the more sensitive Ts9 SFV-Rluc. The readout was by immunostaining of dsRNA (Figures 4A and 4B) and luciferase assay (not shown), respectively. The cellular NMD factors tested were Upf2, Upf3A, Upf3B, Smg1, Smg5, Smg6, and Smg7. These were depleted individually and in various combinations. Reverse transcription qualitative polymerase chain reaction (RT-qPCR) analysis showed that the depletion efficiency of Upf1, Smg5, Smg6, and Smg7 was sufficient to strongly upregulate the mRNA levels of known endogenous mRNAs targeted by NMD (Figure S3).

A substantial increase in the level of dsRNA (and luciferase counts) 4 hr postinfection was evident in cells depleted of Smg5 and Smg7 (Figures 4A and 4B). These factors are known to form a heterodimeric adaptor complex that binds to phosphorylated Upf1 and directs mRNAs to exonucleolytic

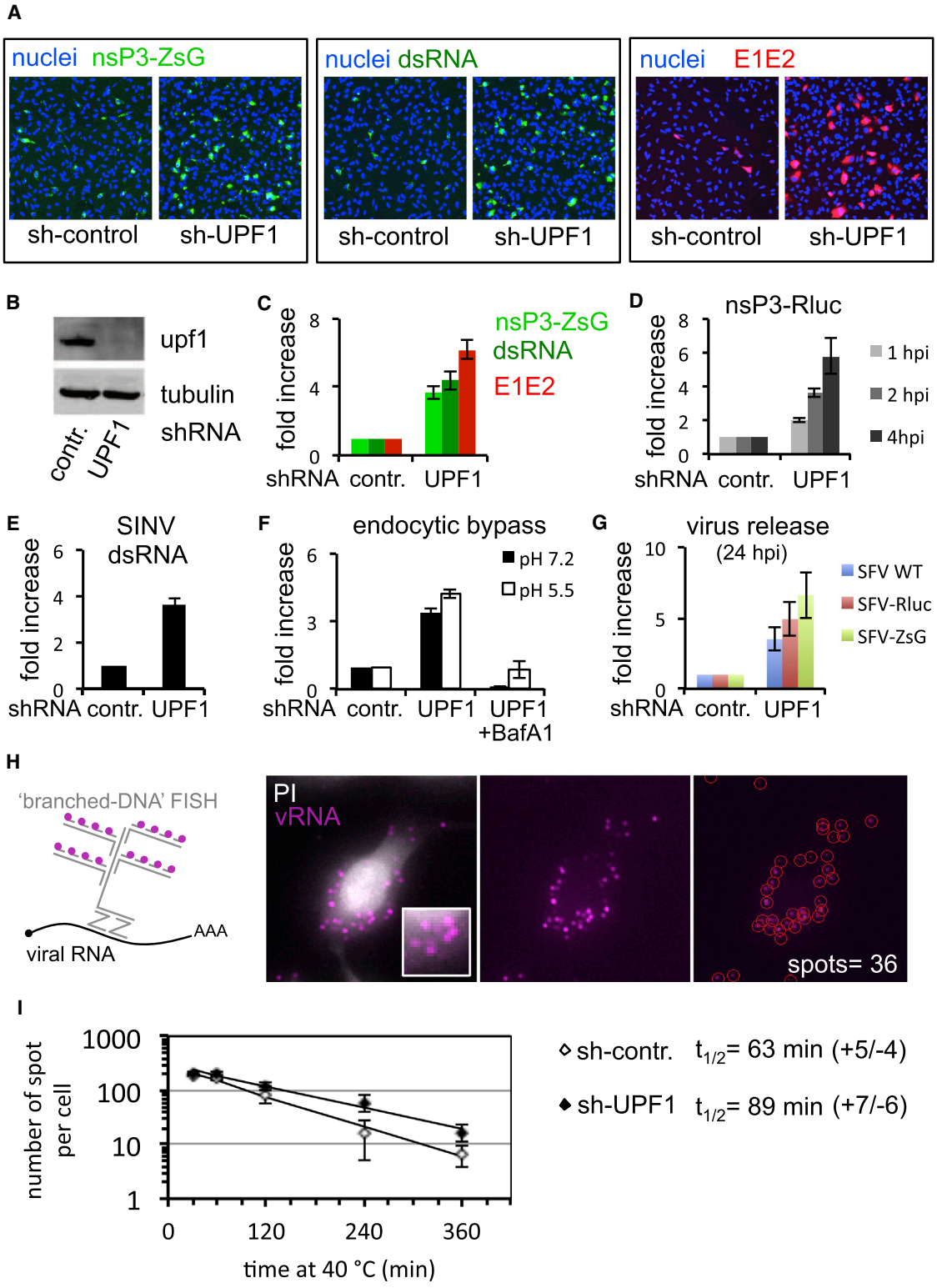

Figure 2. Upf1 Restricts Alphavirus Replication in HeLa Cells

(A) Images of cells treated with indicated shRNAs and infected with SFV-ZsG for 4 hr. The viral products are visualized by direct fluorescence (nsP3-ZsG) or immunofluorescence (dsRNA and E1E2).

(B) Western blot analysis of the Upf1 knockdown (KD) efficiency after shRNA treatment (from the same experiment shown in A).

(legend continued on next page)

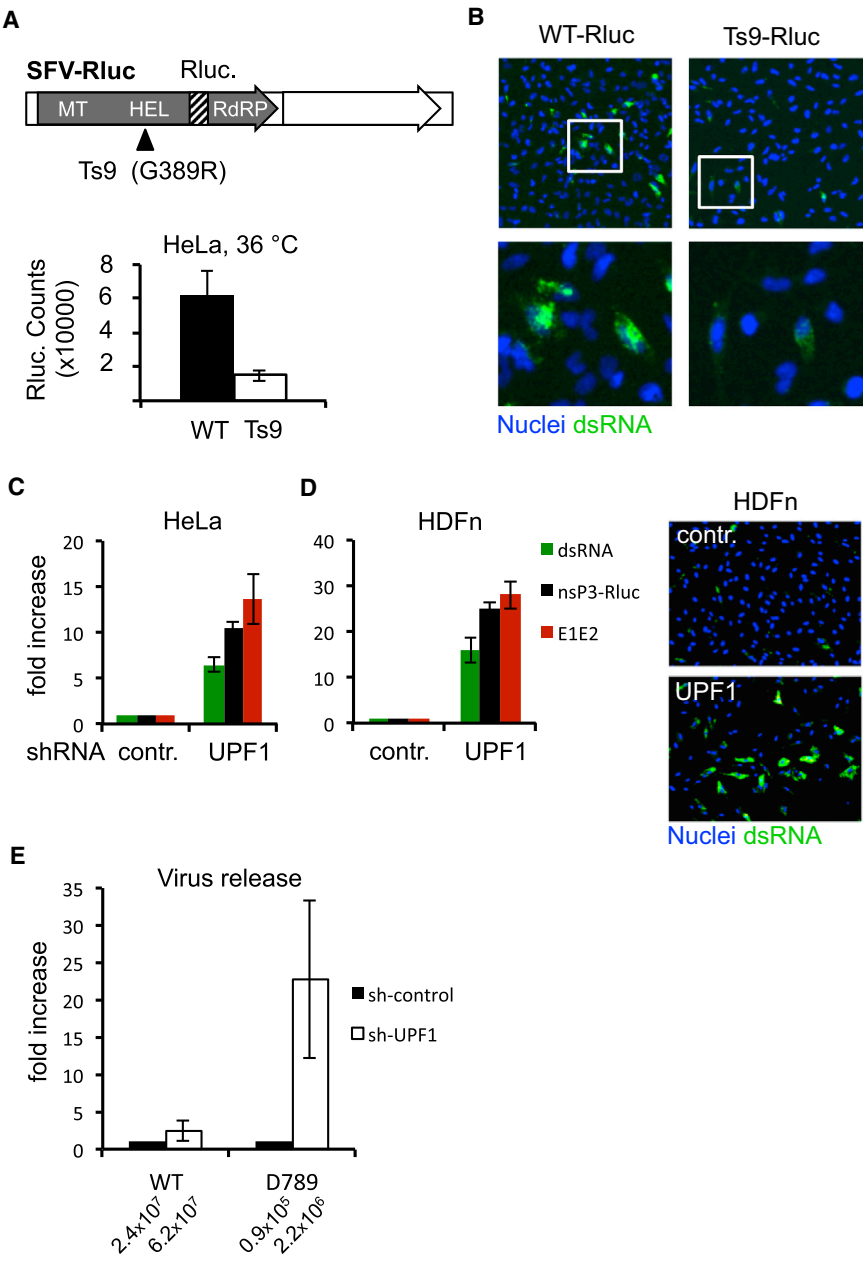

Figure 3. Impairing Virus Replication Increases the Sensitivity to Upf1 in HeLa and Primary Cells

(A) Schematic representation of SFV-Rluc-Ts9 genome and efficiency of virus replication at 36°C as measured by renilla luciferase assay. The mutation that confers the temperature-sensitive phenotype is indicated.

(B) Immunostaining of dsRNA in HeLa cells infected for 4 hr with the indicated viruses at 36°C.

(C and D) Efficiency of nsPs, dsRNA, and E1E2 production in HeLa (C) and neonatal human dermal fibroblast (HDFn) (D) cells infected with SFV-Rluc-Ts9 at 36°C for 4 hr. Representative images of HDFn treated with indicated shRNAs and immunostained for dsRNA at 4 hr post-infection.

(E) Virus production after Upf1 depletion in HeLa cells infected with indicated viruses for 24 hr.

degradation (Loh et al., 2013; Unterholzner and Izaurralde, 2004). In contrast, depletion of the endonuclease Smg7 (Eberle et al., 2009; Huntzinger et al., 2008) had no effect (Figures 4A and 4B).

Thus, despite being effective in targeting multiple cellular NMD substrates for degradation (Figure S3A), Smg6 had no effect on SFV infection. A different sensitivity for the depletion of Smg6 and Smg7 was observed for the cellular noncoding RNA GAS5 and DCLK1, both targets of NMD (Figure S3B, red box) (Tani et al., 2013). The level of depletion of Upf2, Upf3A, and Upf3B, each independently or in combinations, may have been not sufficient to affect virus infection, and thus no conclusions could be drawn from these negative results. The shRNA treatment to deplete Smg1 was toxic for the cells and had to be excluded from further analysis (not shown).

In summary, our results indicated that in addition to Upf1, the suppression of viral genome replication and amplification early in infection involved Smg5 and Smg7.

Does the Length of the Genomic 3′ UTR Influence Replication?

Cellular mRNAs with long 3′ UTR sequences can be targeted by NMD, even if they do not contain premature stop codons (PTCs) (Bühler et al., 2006). Due to the presence of the subgenomic RNA, the 3′ UTR of the alphavirus genomes is extremely long (~4,000 nt). To test whether the long 3′ UTR made the viral genome vulnerable to NMD, we produced virus-like particles in which the length on the genomic 3′ UTR was reduced to 62 nucleotides (Figure S3C). Despite the substantial shortening, the depletion of Upf1 still caused an increase in the ZsG fluorescence comparable to that obtained for viruses that have a full-length 3′ UTR (Figures 4C and 4D). Thus, unlike

(C–E) Relative infection levels in cells treated with indicated shRNAs and infected with SFV-ZsG (C), SFV-RLuc (D), or SINV (E). The indicated viral products were monitored by image-based (C and E) or renilla luciferase (D) assays.

(F) Effect of Upf1 KD in cells infected with SFV by low-pH-induced fusion with the plasma membrane. Infected cells are detected by dsRNA immunostaining.

(G) Viral yields after Upf1 KD (24 hpi).

(H) Image-based detection of single incoming viral genomes by branched-DNA FISH in cells infected with SFV ts9 at 40°C for 30 min. After fixation, cells were visualized by propidium iodide staining (PI).

(I) Kinetics of genomic RNA decay in cells treated with shRNA against UPF1 or luciferase (sh-contr.) (see also Figure S2).

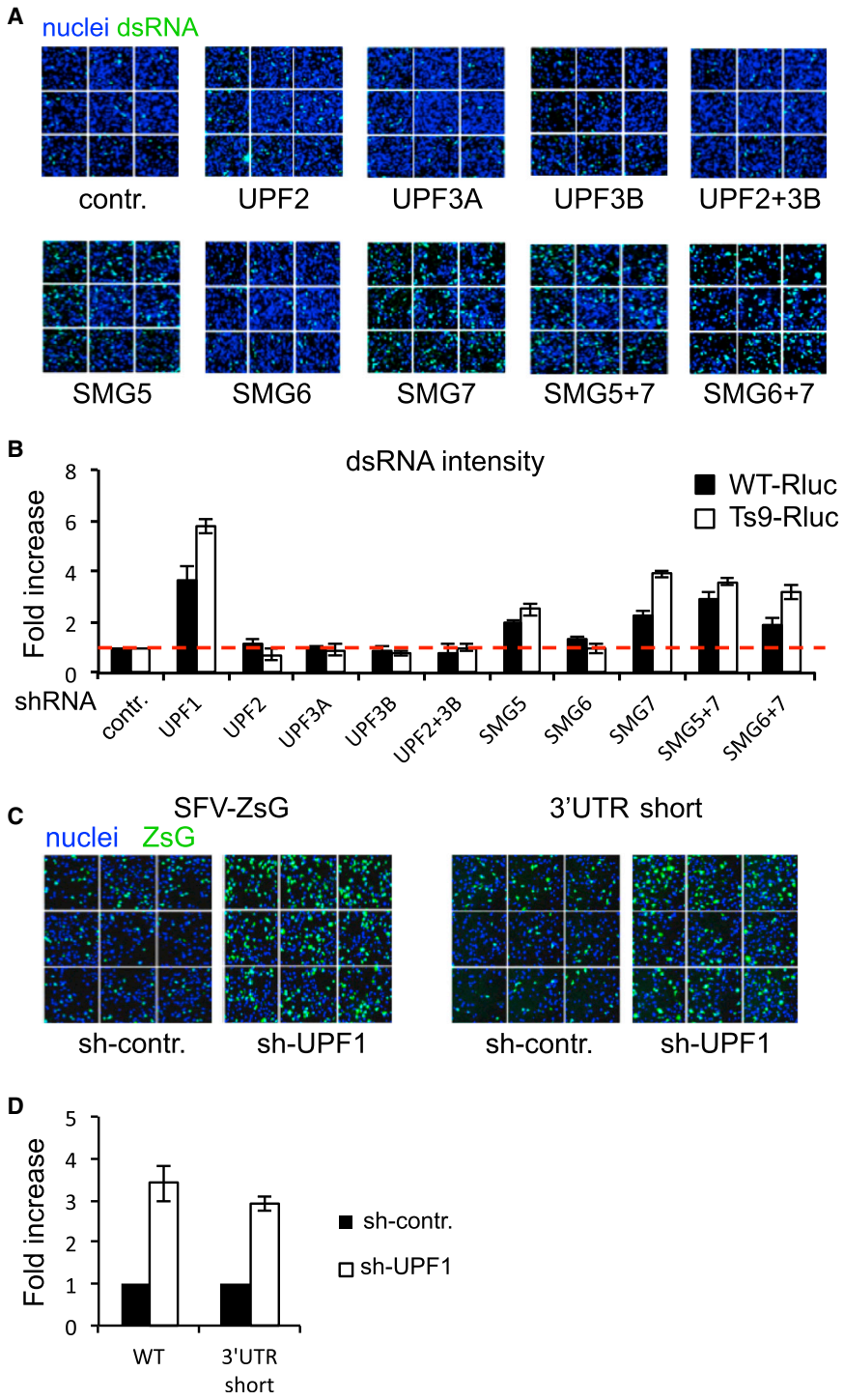

Figure 4. Depletion of Smg5 and Smg7 Increases SFV Infection

(A) Representative images of dsRNA-immunostained HeLa cells infected with SFV for 4 hr. Cells were pretreated with indicated shRNAs as in Figure 2. Nine images were acquired for each sample.

(B) Relative infection in cells treated as in (A) and processed by quantitative image analysis.

(C) Single-molecule fluorescence imaging of HeLa cells pretreated with indicated shRNAs and infected for 4 hr with equivalent amounts of SFV-ZsG (left panel) or SFV-ZsG virus-like particles with a short 3′ UTR (right panel).

(D) Quantification of the intensity of ZsG fluorescence in the infected cells as in (C) (error bars represent the standard deviation of three independent experiments) (see also Figure S3).

cellular mRNA, the long SFV 3′ UTR does not appear to be the feature that renders the viral RNA sensitive to Upf1-mediated destabilization.

DISCUSSION

Our main finding was that the depletion of Upf1 and two of its cofactors in the NMD process, Smg5 and Smg7, increased the infection of SFV in tissue culture cells. The results indicated that Upf1 and these cofactors suppress the replication and amplification of the incoming viral RNA after its uncoating in the cytosol by inducing degradation of the incoming +-RNA. As a consequence, all later steps in the replication cycle are also inhibited. Similar results were obtained for SINV, another alphavirus. In primary human fibroblasts, the effect of Upf1 depletion was even stronger than in the HeLa cells used in the initial screen. Upf1 depletion did not affect infection by two negative-stranded RNA viruses of the paramyxo- and bunyavirus families.

It was apparent that Upf1 and a process related to NMD serve as an intrinsic mechanism of innate immunity against +-RNA viruses in animal cells. The incoming viral RNA is apparently recognized soon after delivery into the cytosol as being "foreign," and all further steps in the infection cycle are restricted. Characteristic for this pathway is that it is constitutive; since it is always present it does not need to be activated by prior exposure to the virus. A similar Upf1-dependent mechanism has recently been discovered in plants where +RNA viruses constitute a large portion of viral pathogens (Garcia et al., 2014). While NMD is generally considered a cellular mRNA quality control pathway devoted to destroying mRNAs with premature stop codons that arise due to splicing errors and other defects, our results in conjunction with the data from Garcia et al. indicate that it may, in addition, play a central role in defending animal as well as plant cells against cytoplasmic pathogens.

While the best-known function of NMD in cells is to eliminate mRNAs that have premature stop codons, an increasing body of evidence indicates that NMD is also responsible for the

degradation of mRNAs that have long 3′ UTR sequences (Bühler et al., 2006; Hogg and Goff, 2010; Yepiskoposyan et al., 2011). Since only the nsPs are synthesized from a single ORF starting at the 5′ end of the genomic +RNA, the 3′ UTR sequence of the SFV genomic RNA encompasses nearly 4,000 nucleotides. It therefore seemed likely that this feature—dictated by the replication strategy of alphaviruses—would make the SFV genome vulnerable to NMD. However, we found that SFV RNAs with a deletion of almost the entire 3′ UTR was restricted by Upf1 to a similar extent as the WT genomic RNA when delivered into the cells by virus-like particles. This demonstrated that the long 3′ UTR was not the major determinant that rendered the SFV RNA vulnerable to NMD. Further studies will be required to highlight the molecular details of how Upf1 interacts with the viral genome.

The genome of alphaviruses is accessible to cytosolic factors like Upf1 and ribosomes probably only during early phases of infection. Minus-strand synthesis is incompatible with simultaneous translation of the positive strand, and since NMD is a translation-dependent process, it could only occur before the onset of replication. When replication starts, the RNA is disengaged from the translation machinery and becomes physically protected within virus-induced membrane-enclosed compartments that limit the access to cytosolic factors such as Upf1. Membrane-associated RNA replication is the hallmark of all studied +RNA viruses (den Boon and Ahlquist, 2010). In some cases, membrane-dependent RNA protection from exogenous RNAase treatment has been demonstrated (Deng et al., 2014; Schwartz et al., 2002).

Later in infection, newly synthesized +RNAs are rapidly packaged into assembling virus capsids. In addition, it is possible that when the viral RNA polymerase has been assembled and replication starts, bound NMD factors are displaced from the genomic +RNA. By competing with Upf1, the viral replicases may be able to protect the viral genome. Consistent with this view, we found that impairing and slowing down the function of the replicase proteins by point mutations or deletions increased the effect of Upf1 depletion. This suggested that reduced replicase activity allows more efficient NMD targeting and degradation of the genomic RNA. In other words, it is likely that the replicases of alphaviruses compete with NMD.

As an alternative to the "competition" model, one or more of the four viral replicase proteins, nsP1–nsP4, might inhibit NMD factors. It is noteworthy that, among the mutant viruses tested in this study, the mutant lacking the C-terminal domain of nsP3 was by far the most sensitive to the presence of Upf1. Investigating the possible role of the nsPs in NMD inhibition is an interesting area for further research.

Viral proteins that inhibit NMD have been identified (Quek and Beemon, 2014). It is likely that various +RNA viruses have also developed mechanisms to avoid recognition and degradation by cellular quality control systems like NMD. Elucidation of these will be an interesting future challenge.

In summary, we provide evidence that NMD restricts alphavirus infection in animal cells by serving as an intrinsic, front-line defense system that suppresses early cytosolic events. Given the conservation of NMD across kingdoms of life and the recent observations in plants (Garcia et al., 2014), we expect that our findings will extend beyond the animal kingdom.

EXPERIMENTAL PROCEDURES

Cells, Viruses, and Antibodies

HeLa and neonatal human dermal fibroblasts (HDFn, ATCC) were grown in DMEM supplemented with 10% of heat-inactivated FBS and Glutamax (Life Technologies). To avoid the accumulation of autofluorescence, all experiments with HDFN were carried out with cells grown for fewer than ten passages. All viruses were propagated in BHK 21 cells (ATCC) grown in MEM supplemented with 2 mM glutamine, 0.2% BSA, and 20 mM HEPES buffer. Virus stocks from cleared supernatants were stored at −80°C. The SFV-ZsG VLPs with 62 nt short 3′ UTRs were produced by standard cloning techniques (see Supplemental Experimental Procedures). The antibodies to detect the capsid and E1E2 envelope proteins of SFV have been described (Singh and Helenius, 1992). Antibody against dsRNA (J2 clone) was purchased from Scicons. Anti-rabbit and anti-mouse Alexa Fluor 488- and 647-conjugated antibodies were purchased from Life Technologies. All antibodies were used at a dilution of 1:1,000.

siRNA Screen

HeLa cells were reverse transfected with siRNA at a final concentration of 20 nM in 384-well plates, using 0.1 μl RNAiMAX (Life Technologies) per well in 100 μl DMEM containing 10% of heat-inactivated FCS, glutamax, and penicillin-streptomycin. The genome-wide siRNA library consisted of four pulled siRNA oligonucleotides per gene (Human ON-TARGETplus, Dharmacon). Seventy-two hours after transfection, cells were infected for 6 hr with SFV-ZsG. Cells were infected with an amount of virus sufficient to obtain an infection rate of ∼30% in control siRNA-treated samples. After fixation in 4% formaldehyde (Sigma) and nuclear staining (Hoechst, Life Technologies), nine images per well were acquired with high-content automated microscopes (ImageXpress, Molecular Devices). Infected cells were detected using Cell Profiler (Carpenter et al., 2006) (http://www.cellprofiler.org) and Advanced Cell Classifier (Horvath et al., 2011) (http://www.acc.ethz.ch/acc.html). The screen was repeated two times independently. The full results of the screen are currently being analyzed and will be published elsewhere.

shRNA Treatments, Virus Infections, and qRT-PCR of Cellular NMD Targets

One day before transfection, 2×10^5 HeLa cells were seeded in each well of 6-well culture plates. The following day, cells were transfected with DNA plasmids encoding the puromycin resistance gene (Brummelkamp et al., 2002) and shRNA sequences against the indicated NMD components (see Supplemental Experimental Procedures). Unless otherwise indicated, cells were infected for 4 hr with a multiplicity of infection (moi) of 5 infection units per cell. A detailed protocol for the qRT-PCR of cellular NMD targets can be found in the Supplemental Experimental Procedures.

Endocytic Bypass and Uncoating Assay

After shRNA treatment as described above, cells were chilled on ice for 10 min and viruses allowed to bind to the plasma membrane for 30 min at 4°C. The inoculum was then removed and virus fusion with the plasma membrane induced by incubating cells for 3 min at 37°C in RPMI medium containing glutamax, 0.2% BSA, and 10 mM MES buffer (pH 5.5) (White et al., 1980). The acidic medium was removed, and cells were incubated in neutral growth medium for 4 hr before fixation and IF analysis or luciferase assay.

For measuring the amount of capsid proteins delivered in the cytoplasm after virus entry, shRNA-treated cells were infected with increasing amount of viruses (moi = 500–1,500) for 40 min in the presence of cycloheximide (Sigma-Aldrich) at a final concentration of 50 μM. After fixation, the viral C-protein was detected by IF analysis.

Half-Life Measurements of SFV Gnomes

The b-DNA FISH KIT for detection of SFV genome was from Panomics. Probes were designed by the manufacturers to detect the central region of nsP3. The FISH staining was performed according to the manufacturer's instructions. After shRNA treatment, HeLa cells in glass-bottom 96-well plates (Matrical) were incubated with viruses (moi = 50) on ice for 45 min. After one wash with infection medium, infected cultures were moved to 40°C for indicated times, fixed with 4% PFA for 30 min, and processed for FISH. The FISH

reaction was performed at 40°C. For more details, see Supplemental Experimental Procedures.

SUPPLEMENTAL INFORMATION

Supplemental Information includes Supplemental Experimental Procedures and three figures and can be found with this article online at http://dx.doi.org/10.1016/j.chom.2014.08.007.

AUTHOR CONTRIBUTIONS

G.B. and A.H. conceived the project. P.H. developed the image analysis software (http://acc.ethz.ch/) and analyzed the data. G.B., C.S., D.Z., G.M., and A.M. performed the experiments. O.M., C.A., A.M. provided reagents and analyzed data. G.B. and A.H. wrote the paper.

ACKNOWLEDGMENTS

We are grateful to members of the Helenius lab for their intellectual contributions and to Tero Ahola and Kirsi Hellström for providing laboratory space and assistance with the SFV-Ts9 experiments. Work by G.B. and A.H. was supported by an Advanced Grant from the ERC. C.S., D.Z., and O.M. were supported by the NCCR RNA & Disease funded by the Swiss National Science Foundation.

Received: April 11, 2014
Revised: July 29, 2014
Accepted: August 19, 2014
Published: September 10, 2014

REFERENCES

Azzalin, C.M., and Lingner, J. (2006). The human RNA surveillance factor UPF1 is required for S phase progression and genome stability. Curr. Biol. *16*, 433–439.

Balistreri, G., Caldentey, J., Kääriäinen, L., and Ahola, T. (2007). Enzymatic defects of the nsP2 proteins of Semliki Forest virus temperature-sensitive mutants. J. Virol. *81*, 2849–2860.

Battich, N., Stoeger, T., and Pelkmans, L. (2013). Image-based transcriptomics in thousands of single human cells at single-molecule resolution. Nat. Methods *10*, 1127–1133.

Brummelkamp, T.R., Bernards, R., and Agami, R. (2002). A system for stable expression of short interfering RNAs in mammalian cells. Science *296*, 550–553.

Bühler, M., Steiner, S., Mohn, F., Paillusson, A., and Mühlemann, O. (2006). EJC-independent degradation of nonsense immunoglobulin-mu mRNA depends on 3′ UTR length. Nat. Struct. Mol. Biol. *13*, 462–464.

Carpenter, A.E., Jones, T.R., Lamprecht, M.R., Clarke, C., Kang, I.H., Friman, O., Guertin, D.A., Chang, J.H., Lindquist, R.A., Moffat, J., et al. (2006). CellProfiler: image analysis software for identifying and quantifying cell phenotypes. Genome Biol. *7*, R100.

Chang, Y.F., Imam, J.S., and Wilkinson, M.F. (2007). The nonsense-mediated decay RNA surveillance pathway. Annu. Rev. Biochem. *76*, 51–74.

Cheng, Z., Muhlrad, D., Lim, M.K., Parker, R., and Song, H. (2007). Structural and functional insights into the human Upf1 helicase core. EMBO J. *26*, 253–264.

den Boon, J.A., and Ahlquist, P. (2010). Organelle-like membrane compartmentalization of positive-strand RNA virus replication factories. Annu. Rev. Microbiol. *64*, 241–256.

Deng, Z., Lehmann, K.C., Li, X., Feng, C., Wang, G., Zhang, Q., Qi, X., Yu, L., Zhang, X., Feng, W., et al. (2014). Structural basis for the regulatory function of a complex zinc-binding domain in a replicative arterivirus helicase resembling a nonsense-mediated mRNA decay helicase. Nucleic Acids Res. *42*, 3464–3477.

Eberle, A.B., Lykke-Andersen, S., Mühlemann, O., and Jensen, T.H. (2009). SMG6 promotes endonucleolytic cleavage of nonsense mRNA in human cells. Nat. Struct. Mol. Biol. *16*, 49–55.

Frolova, E.I., Gorchakov, R., Pereboeva, L., Atasheva, S., and Frolov, I. (2010). Functional Sindbis virus replicative complexes are formed at the plasma membrane. J. Virol. *84*, 11679–11695.

Garcia, D., Garcia, S., and Voinnet, O. (2014). Nonsense-mediated decay serves as a general viral restriction mechanism in plants. Cell Host & Microbe *16*, this issue, 391–402.

Helenius, A., Kartenbeck, J., Simons, K., and Fries, E. (1980). On the entry of Semliki forest virus into BHK-21 cells. J. Cell Biol. *84*, 404–420.

Hogg, J.R., and Goff, S.P. (2010). Upf1 senses 3'UTR length to potentiate mRNA decay. Cell *143*, 379–389.

Horvath, P., Wild, T., Kutay, U., and Csucs, G. (2011). Machine learning improves the precision and robustness of high-content screens: using nonlinear multiparametric methods to analyze screening results. J. Biomol. Screen. *16*, 1059–1067.

Huntzinger, E., Kashima, I., Fauser, M., Saulière, J., and Izaurralde, E. (2008). SMG6 is the catalytic endonuclease that cleaves mRNAs containing nonsense codons in metazoan. RNA *14*, 2609–2617.

Hurt, J.A., Robertson, A.D., and Burge, C.B. (2013). Global analyses of UPF1 binding and function reveal expanded scope of nonsense-mediated mRNA decay. Genome Res. *23*, 1636–1650.

Isken, O., Kim, Y.K., Hosoda, N., Mayeur, G.L., Hershey, J.W., and Maquat, L.E. (2008). Upf1 phosphorylation triggers translational repression during nonsense-mediated mRNA decay. Cell *133*, 314–327.

Kashima, I., Yamashita, A., Izumi, N., Kataoka, N., Morishita, R., Hoshino, S., Ohno, M., Dreyfuss, G., and Ohno, S. (2006). Binding of a novel SMG-1-Upf1-eRF1-eRF3 complex (SURF) to the exon junction complex triggers Upf1 phosphorylation and nonsense-mediated mRNA decay. Genes Dev. *20*, 355–367.

Keränen, S., and Kääriäinen, L. (1974). Isolation and basic characterization of temperature-sensitive mutants from Semliki Forest virus. Acta Pathol Microbiol Scand B Microbiol Immunol. *82*, 810–820.

Keränen, S., and Kääriäinen, L. (1979). Functional defects of RNA-negative temperature-sensitive mutants of Sindbis and Semliki Forest viruses. J. Virol. *32*, 19–29.

Kervestin, S., and Jacobson, A. (2012). NMD: a multifaceted response to premature translational termination. Nat. Rev. Mol. Cell Biol. *13*, 700–712.

Loh, B., Jonas, S., and Izaurralde, E. (2013). The SMG5-SMG7 heterodimer directly recruits the CCR4-NOT deadenylase complex to mRNAs containing nonsense codons via interaction with POP2. Genes Dev. *27*, 2125–2138.

Lykke-Andersen, J., and Bennett, E.J. (2014). Protecting the proteome: Eukaryotic cotranslational quality control pathways. J. Cell Biol. *204*, 467–476.

Meier, R., Franceschini, A., Horvath, P., Tetard, M., Mancini, R., von Mering, C., Helenius, A., and Lozach, P.Y. (2014). Genome-Wide Small Interfering RNA Screens Reveal VAMP3 as a Novel Host Factor Required for Uukuniemi Virus Late Penetration. J. Virol. *88*, 8565–8578.

Paillusson, A., Hirschi, N., Vallan, C., Azzalin, C.M., and Mühlemann, O. (2005). A GFP-based reporter system to monitor nonsense-mediated mRNA decay. Nucleic Acids Res. *33*, e54.

Panas, M.D., Varjak, M., Lulla, A., Eng, K.E., Merits, A., Karlsson Hedestam, G.B., and McInerney, G.M. (2012). Sequestration of G3BP coupled with efficient translation inhibits stress granules in Semliki Forest virus infection. Mol. Biol. Cell *23*, 4701–4712.

Pohjala, L., Utt, A., Varjak, M., Lulla, A., Merits, A., Ahola, T., and Tammela, P. (2011). Inhibitors of alphavirus entry and replication identified with a stable Chikungunya replicon cell line and virus-based assays. PLoS ONE *6*, e28923.

Quek, B.L., and Beemon, K. (2014). Retroviral strategy to stabilize viral RNA. Curr. Opin. Microbiol. *18*, 78–82.

Schwartz, M., Chen, J., Janda, M., Sullivan, M., den Boon, J., and Ahlquist, P. (2002). A positive-strand RNA virus replication complex parallels form and function of retrovirus capsids. Mol. Cell *9*, 505–514.

Schweingruber, C., Rufener, S.C., Zünd, D., Yamashita, A., and Mühlemann, O. (2013). Nonsense-mediated mRNA decay - mechanisms of substrate mRNA recognition and degradation in mammalian cells. Biochim. Biophys. Acta *1829*, 612–623.

Singh, I., and Helenius, A. (1992). Role of ribosomes in Semliki Forest virus nucleocapsid uncoating. J. Virol. *66*, 7049–7058.

Spuul, P., Balistreri, G., Kääriäinen, L., and Ahola, T. (2010). Phosphatidylinositol 3-kinase-, actin-, and microtubule-dependent transport of Semliki Forest Virus replication complexes from the plasma membrane to modified lysosomes. J. Virol. *84*, 7543–7557.

Tani, H., Torimura, M., and Akimitsu, N. (2013). The RNA degradation pathway regulates the function of GAS5 a non-coding RNA in mammalian cells. PLoS ONE *8*, e55684.

Unterholzner, L., and Izaurralde, E. (2004). SMG7 acts as a molecular link between mRNA surveillance and mRNA decay. Mol. Cell *16*, 587–596.

White, J., and Helenius, A. (1980). pH-dependent fusion between the Semliki Forest virus membrane and liposomes. Proc. Natl. Acad. Sci. USA *77*, 3273–3277.

White, J., Kartenbeck, J., and Helenius, A. (1980). Fusion of Semliki forest virus with the plasma membrane can be induced by low pH. J. Cell Biol. *87*, 264–272.

Yan, N., and Chen, Z.J. (2012). Intrinsic antiviral immunity. Nat. Immunol. *13*, 214–222.

Yepiskoposyan, H., Aeschimann, F., Nilsson, D., Okoniewski, M., and Mühlemann, O. (2011). Autoregulation of the nonsense-mediated mRNA decay pathway in human cells. RNA *17*, 2108–2118.

Zünd, D., Gruber, A.R., Zavolan, M., and Mühlemann, O. (2013). Translation-dependent displacement of UPF1 from coding sequences causes its enrichment in 3′ UTRs. Nat. Struct. Mol. Biol. *20*, 936–943.

Cell Host & Microbe, Volume *16*

Supplemental Information

The Host Nonsense-Mediated mRNA Decay Pathway Restricts Mammalian RNA Virus Replication

Giuseppe Balistreri, Peter Horvath, Christoph Schweingruber, David Zünd, Gerald McInerney, Andres Merits, Oliver Mühlemann, Claus Azzalin, and Ari Helenius

Supplementary Experimental procedures

shRNA plasmids used in the study

Target Factor	Target Sequence	References
UPF1	5'-GATGCAGTTCCGCTCCATT-3'	(Azzalin and Lingner, 2006)
UPF2	5'-GAAGTTGGTACGGGCACTC-3'	(Kashina et al., 2006)
UPF3A	5’-GACAGATAAACAGAAGAAA-3’	this study
UPF3B	5’-GGTGGTAATTCGAAGATTA-3’	(Yepiskoposyan et al., 2011)
SMG5	5'-GAAGGAAATTGGTTGATAC-3'	(Okada-Katsuhata et al., 2012)

Primers used for qRT-PCR of endogenous NMD targets

Gene Name	Assay Type	Reference Transcripts	Amplicon Region	Oligonucleotide Sequences Fluorophores	References
UPF1	TaqMan®	NM_002911.3	exon 3	5'-TGCAACGGACGTGGAAATAC-3' 5'-ACCTCTTTGCATTTTGCCCTC-3' 5'-FAM-TCTGGCAGCCACATTGTAAATCACCTTG-BHQ1-3'	(Yepiskoposyan et al., 2011)
UPF2	SYBR® Green	NM_015542.3, NM_080599.2	3'-UTR	5'-AGCAGCACGTGTCATTTC-3' 5'-TGTGTCCACTGCTCTCATTC-3'	this study
UPF3A	SYBR® Green	NM_080687, NM_023011	exon 1 / exon 2	5'-TGTCGGCCCTAGAAGTGCAG-3' 5'-CGGATGACCACCTTGCTCAG-3'	this study
UPF3B	SYBR® Green	NM_023010, NM_080632	exon 9 / exon 10	5'-GTACATTGCCCAAGCGTTCTG-3' 5'-AAGTATGCGCTCCTGATCTCG-3'	this study
SMG5	TaqMan®	NM_015327.1	exon 16 / exon 17	5'-GTCAGCATTGCCCAGTCTGA-3' 5'-AGCCTGTTCCGACGAGCTT-3' 5'-FAM-AGGCACAGTTCCGAATGGCACA-BHQ1-3'	(Yepiskoposyan et al., 2011)
SMG6	TaqMan®	NM_017575.4	exon 16 / exon 17	5'-GACACCAACGGCTTCATTGA-3' 5'-CAGGCCGTCCAGCTCATT-3' 5'-FAM-CTGGTGGTGCCCCTCATCGTGAT-BHQ1-3'	(Yepiskoposyan et al., 2011)
SMG7	TaqMan®	NM_173156.2	exon 17 / exon 18	5'-TCTTCCGTCCAGAGCAGGAT-3' 5'-AGCTCTGAGGGCTTCTCCAAT-3' 5'-FAM-CTGTACCCAGAATGCCGTTTGAGAAATCC-BHQ1-3'	(Yepiskoposyan et al., 2011)

Gene Name	Assay Type	Reference Transcripts	Amplicon Region	Oligonucleotide Sequences Fluorophores	References
DCLK1	TaqMan®	NM_004734.2	exon 14 / exon 15	FAM, MGB	this study
GAS5	SYBR® Green	ENSG00000234741	exon 2 – exon 7	5'-GCACCTTATGGACAGTTG-3' 5'-GGAGCAGAACCATTAAGC-3'	this study

Gene Name	Assay Type	Reference Transcripts	Amplicon Region	Oligonucleotide Sequences Fluorophores	References
ACTB	SYBR® Green	NM_001101.3	exon 5 / exon 6	5'-TCCATCATGAAGTGTGACGT-3' 5'-TACTCCTGCTTGCTGATCCAC-3'	this study
ACTB	TaqMan®	NM_001101.3	exon 5 / exon 6	5'-CTGGCACCCAGCACAATG-3' 5'-GCCGATCCACACGGAGTACT-3' 5'-FAM-ATCAAGATCATTGCTCCTCCTGAGCGC-BHQ1-3'	(Metze et al., 2013)

Supplementary references

Azzalin, C.M., and Lingner, J. (2006). The human RNA surveillance factor UPF1 is required for S phase progression and genome stability. Current biology : CB *16*, 433-439.

Metze, S., Herzog, V.A., Ruepp, M.D., and Muhlemann, O. (2013). Comparison of EJC-enhanced and EJC-independent NMD in human cells reveals two partially redundant degradation pathways. Rna *19*, 1432-1448.

Okada-Katsuhata, Y., Yamashita, A., Kutsuzawa, K., Izumi, N., Hirahara, F., and Ohno, S. (2012). N- and C-terminal Upf1 phosphorylations create binding platforms for SMG-6 and SMG-5:SMG-7 during NMD. Nucleic acids research *40*, 1251-1266.

Yepiskoposyan, H., Aeschimann, F., Nilsson, D., Okoniewski, M., and Muhlemann, O. (2011). Autoregulation of the nonsense-mediated mRNA decay pathway in human cells. Rna *17*, 2108-2118.

Production of SFV-ZsG with short 3'-UTR

The SFV-ZsG VLPs with 62 nt short 3'UTR were produced by truncation of the RNA sequence between the stop codon of nsP4 and a naturally occurring Hind III cleavage in position 11384 of the cDNA clone pSFV4. The deletion was made by PCR using pHelper1 plasmid as template (Liljestrom and Garoff, 1991) and Phusion DNA polymerase (Thermo Scientific) as enzyme. Obtained PCR product was cut with Hind III, ligated with T4 DNA ligase and used for transformation of E.coli strain XL-10. Finally, the Bgl II to Spe I restriction fragment from the obtained plasmid was used to substitute corresponding fragment of pSFV-ZsG infectious clone (Spuul et al., 2010).

shRNA treatments and virus infections

One day before transfection, $2x10^5$ HeLa cells were seeded in each well of 6-well culture plates. The following day, cells were transfected with DNA plasmids encoding the puromycin resistance gene (Brummelkamp et al., 2002) and shRNA sequences against the indicated NMD components (see supplementary experimental procedures) using 4ul/well of Dreamfect (OZ Biosciences) or Lipofectamine-2000 (Life Technologies) according to manufacturer instructions.
Five hours after transfection, the transfection medium was replaced with DMEM containing 10% heat-inactivated FBS and glutamax, and cells incubated at 37°C. 24 hours after transfection, positively transfected cells were selected with puromycin at a final concentration of 1.75 ug/ml. Two days later the selection medium was removed and cells were trypsinized and transferred to 6-well plates for qRT-PCR analysis and virus production assays, and to 96-well plates for image- or luciferase-based infection assays. To obtain sufficient transfection efficiency in primary cells, $1x10^6$ HDFn cells were electroporated with 2.5 ug of plasmid DNA using the Amaxa electroporator (protocol U23) and the respective HDFn-electroporation buffer (Lonza). Unless otherwise indicated, cells were infected for 4 hours with a multiplicity of infection of 5 infection units per cell in DMEM, 0.2% BSA, glutamax and 20 mM HEPES.

qRT-PCR of cellular NMD targets

Total RNA was extracted with Trizure (Bioline) or Trizol (Life Technologies) according to manufactures instructions and treated with recombinant DNase I (Roche, Switzerland) for 20 min before re-extracting total RNA with acidic phenol (Sigma Aldrich) and concentration by 2-propanol precipitation. The RNA was finally resuspended and stabilized in 1 mM trisodium citrate pH 6.5 and its integrity was visually assessed on agarose gels by ethidium bromide staining.
cDNA was reverse transcribed from 1 ug DNase-treated total RNA using random hexamer primers (Microsynth, Switzerland) and AffinityScript Multiple-Temperature Reverse Transcriptase (Agilent Technologies). PCR reactions used the assay oligonucleotides described in Supplementary Experimental Procedures in either Brilliant III Ultra Fast QPCR Master Mix for TaqMan® assays or Brilliant III Ultra Fast SYBR® Green QPCR Master Mix and were pipetted using a CAS1200 robot (Corbett Life Science). Real-time fluorescence data were recorded on a Rotorgene 6200 (Corbett Life Science) and CT values were extracted using the

accompanying software. CT values of replicates were averaged before relative expression levels were calculated according to the ΔΔCT method (Pfaffl et al., 2001) and errors were calculated by propagation of uncertainty of the CT values.

Half-life measurements of SFV gnomes

For each sample, 36 images were acquired using an epifluorescence automated microscope (CellInsight, Thermo Scientific) and a 20x objective. Image analysis was performed with the Mosaic plug-in of Fiji (Image J). For estimation of the RNA half-life, the exponential regression was performed using Microsoft Excel. The exponential decay constant λ was extracted from the slope, and the standard error of the slope of the regression fit using Excel's LOGEST function, and converted to half-life values by $T_{1/2} = \ln(2) / (\lambda$ +/- se_ $\lambda)$.

References

Brummelkamp, T.R., Bernards, R., and Agami, R. (2002). A system for stable expression of short interfering RNAs in mammalian cells. Science *296*, 550-553.
Spuul, P., Balistreri, G., Kaariainen, L., and Ahola, T. (2010). Phosphatidylinositol 3-kinase-, actin-, and microtubule-dependent transport of Semliki Forest Virus replication complexes from the plasma membrane to modified lysosomes. J Virol *84*, 7543-7557.

Figure S1, related to Figure 1. Image analysis and reproducibility of the genome wide siRNA screen. (A) Representative image of HeLa cells infected with SFV-ZsG for 6 hours. Image analysis performed with Cell Profiler is used to trace the perimeter of the nuclei visualized by Hoechst staining. The traced area is expanded and the fluorescent signal of nsP3-ZsG quantified to identify infected cells. (B) Correlation of the infection values obtained for all genes KD in two independent repetitions. GW-1 = genome-wide siRNA screen repetition 1; GW-2 = genome-wide siRNA screen repetition 2. The black mark indicates the infection values obtained for the UPF1 depletion. (related to Figure 1)

Figure S2, related to Figure 2. UPF1 depletion does not affect virus penetration. (A) Schematic representation of viral genome uncoating after virus entry by endocytosis or of low-pH induced fusion at the plasma membrane (endocytic bypass). (B) Immunofluorescence assay of virus capsid proteins to measure uncoating in HeLa cells infected with increasing amount of virus for 40 min at 37 °C, in the presence of cycloheximide. Images are acquired with a 20x objective using a high content automated microscope (Image Express, Molecular Devices). (C) Quantification of virus uncoating by image analysis in HeLa cells pre-treated with indicated shRNAs as in figure 2 and infected with SFV for 40 min in the presence of cycloheximide (m.o.i. 500). Bafilomycin A1, an inhibitor of endosomal acidification, was used at a final concentration of 20 nM. (D) Fluorescence imaging of HeLa cells co-transfected with plasmids encoding the indicated shRNAs and a wild-type (WT) or helicase-inactive (K509Q) shRNA-resistant and HA-tagged UPF1 protein. Five days after transfection cells were infected with SFV ZsG (green) (m.o.i. 5) for 4 hours. The UPF1 protein levels were monitored by immunofluorescence using an antibody against the HA-tag (red). The quantification of the ZsG fluorescence is shown in the lower panel. (E) Representative images and image analysis of HeLa cells processed for single molecule RNA FISH. After shRNA treatments, cells were infected with SFV Ts9 (m.o.i. 50) at 40 °C for indicated times. Cells were visualized by propidium iodide.

Figure S3, related to Figure 4. Knockdown of NMD components stabilizes cellular targets of NMD. (A) QRT-PCR analysis of the mRNA levels of cellular NMD targets in HeLa cells pre-treated with shRNAs against indicated NMD components. (B) Same as in A; note the inverse sensitivity of DCLK1 and GAS5 RNA levels to the KD of SMG6 and SMG7 (red box). Values are the average of two independent experiments and error bars represent the standard error. (C) Schematic representation of the genome of SFV-ZsG and SFV-ZsG virus-like particles with short 3'UTR.

A

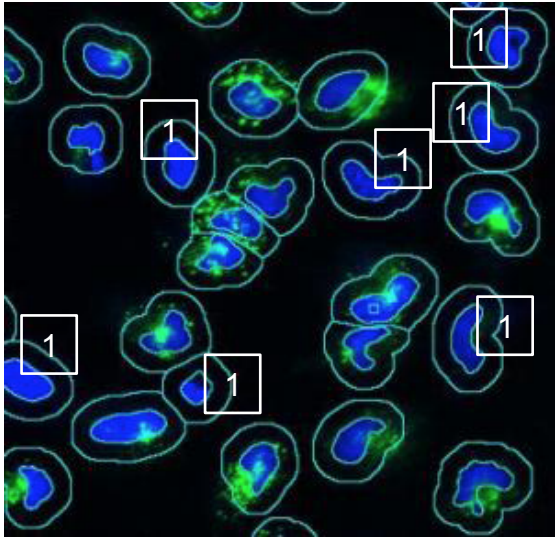

1 = non infected

B

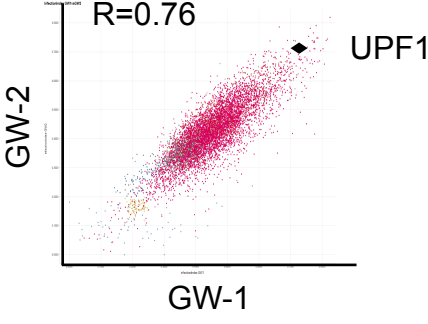

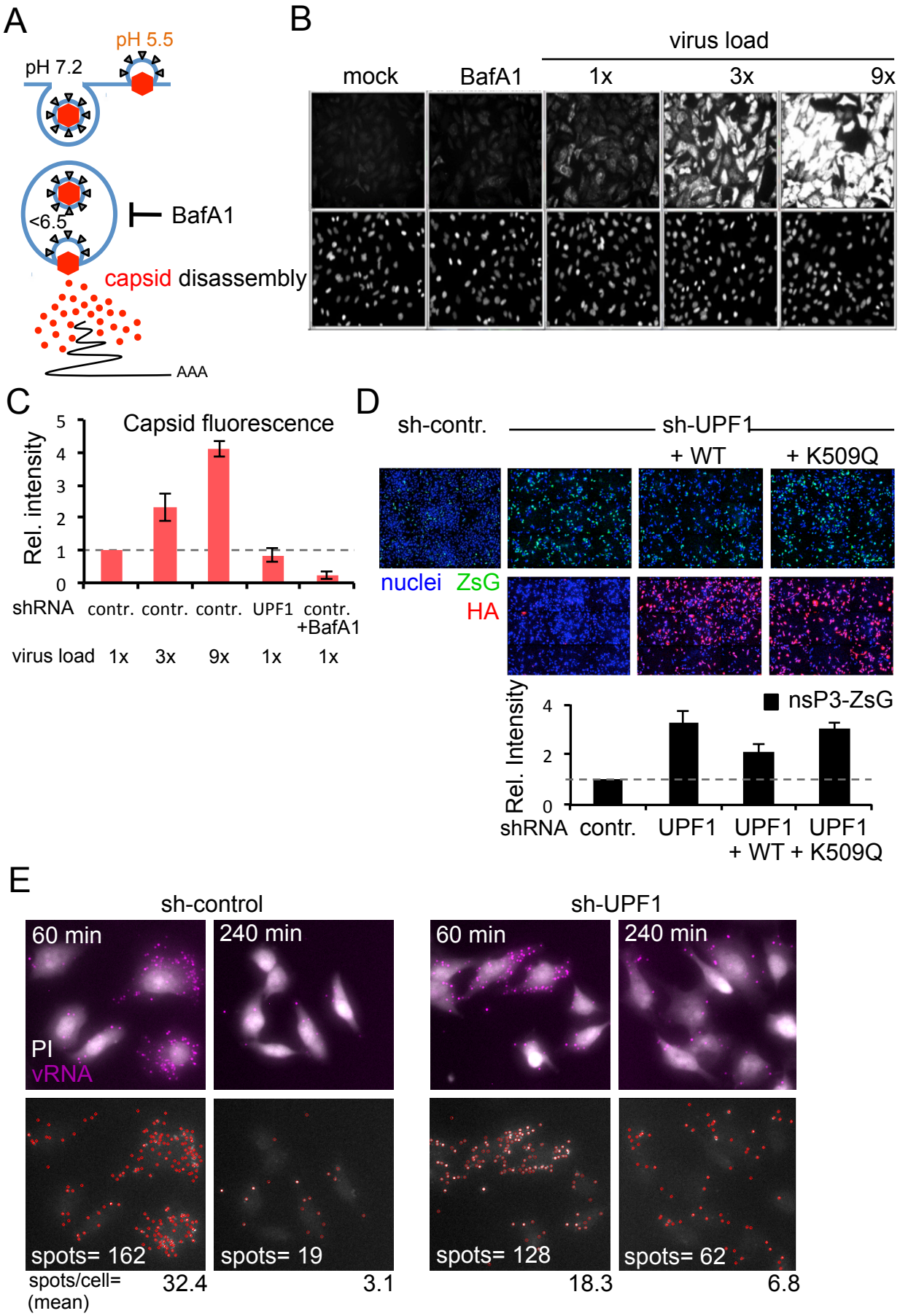
A
pH 7.2
pH 5.5
<6.5
BafA1
capsid disassembly
AAA
B
virus load
mock
BafA1
1x
3x
9x
C
Capsid fluorescence
Rel. intensity
5
4
3
2
1
0
shRNA
contr.
contr.
contr.
UPF1
contr.
+BafA1
virus load
1x
3x
9x
1x
1x
D
sh-contr.
sh-UPF1
+ WT
+ K509Q
nuclei
ZsG
HA
nsP3-ZsG
Rel. Intensity
4
2
0
shRNA
contr.
UPF1
UPF1
+ WT
UPF1
+ K509Q
E
sh-control
sh-UPF1
60 min
240 min
60 min
240 min
PI
vRNA
spots= 162
spots= 19
spots= 128
spots= 62
spots/cell=
(mean)
32.4
3.1
18.3
6.8

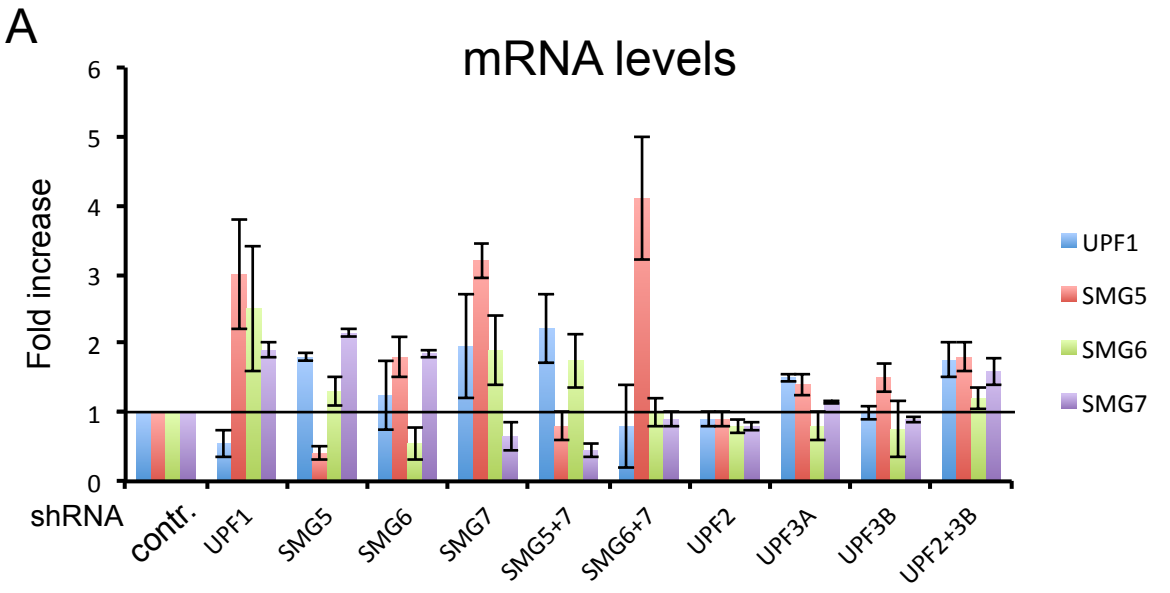
A
mRNA levels
Fold increase
0
1
2
3
4
5
6
shRNA
contr.
UPF1
SMG5
SMG6
SMG7
SMG5+7
SMG6+7
UPF2
UPF3A
UPF3B
UPF2+3B
UPF1
SMG5
SMG6
SMG7

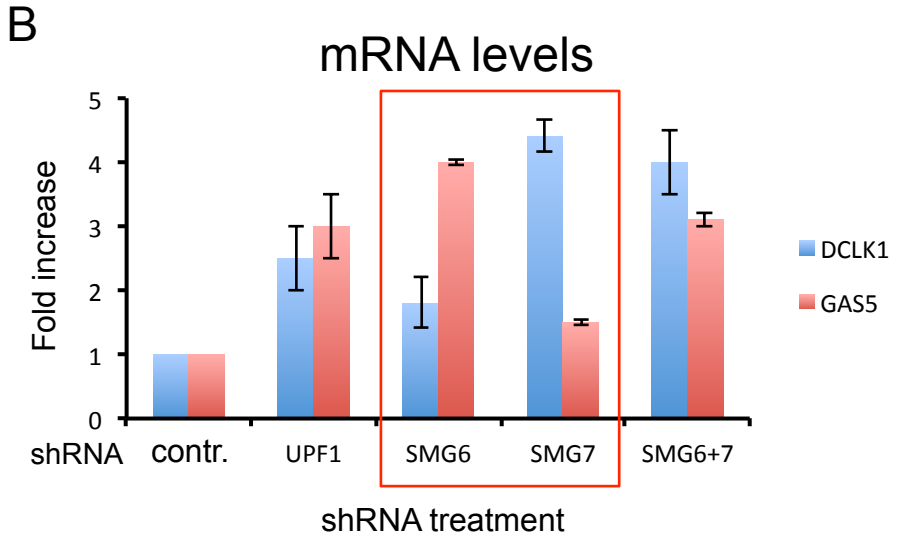
B
mRNA levels
Fold increase
0
1
2
3
4
5
shRNA
contr.
UPF1
SMG6
SMG7
SMG6+7
shRNA treatment
DCLK1
GAS5

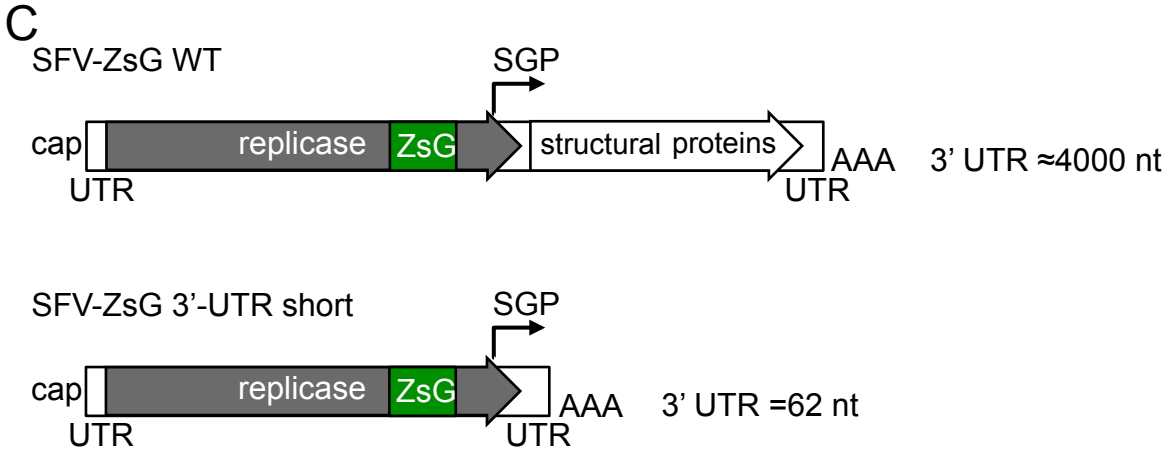
C
SFV-ZsG WT
SGP
cap
replicase
ZsG
structural proteins
AAA
UTR
UTR
3' UTR ≈4000 nt
SFV-ZsG 3'-UTR short
SGP
cap
replicase
ZsG
AAA
UTR
UTR
3' UTR =62 nt